Interactions between conserved domains within homodimers in the BIG1, BIG2, and GBF1 Arf guanine nucleotide exchange factors.

Odile Ramaen, Alexandra Joubert, Philip Simister, Naïma Belgareh-Touzé, Maria Conception Olivares-Sanchez, Jean-Christophe Zeeh, Sophie Chantalat, Marie-Pierre Golinelli-Cohen, Catherine L Jackson, Valérie Biou, et al.

INTERACTIONS BETWEEN CONSERVED DOMAINS WITHIN HOMODIMERS IN THE BIG1, BIG2 AND GBF1 ARF GUANINE NUCLEOTIDE EXCHANGE FACTORS.

Odile Ramaen[1], Alexandra Joubert[1], Philip Simister[1], Naïma Belgareh-Touzé[2], Maria Conception Olivares-Sanchez[1], Jean-Christophe Zeeh[1], Sophie Chantalat[1] , Marie-Pierre Golinelli-Cohen[1], Catherine L. Jackson[1], Valérie Biou[1], Jacqueline Cherfils[1]

[1] Laboratoire d'Enzymologie et Biochimie Structurales, CNRS, 91198 Gif-sur-Yvette, France
[2] Institut Jacques Monod-CNRS Universités Paris VI et VII, 75251 Paris , France

Corresponding author : Jacqueline Cherfils, Laboratoire d'Enzymologie et Biochimie Structurales, CNRS, avenue de la Terrasse, 91198 Gif-sur-Yvette Cedex, France. Email: cherfils@lebs.cnrs-gif.fr
Tel: +33 1 6982 3492, Fax: +33 1 6982 3129

Guanine nucleotide exchange factors carrying a Sec7 domain (ArfGEFs) activate the small GTP-binding protein Arf, a major regulator of membrane remodeling and protein trafficking in eukaryotic cells. Only two of the seven subfamilies of ArfGEFs –GBF and BIG– are found in all eukaryotes. In addition to the Sec7 domain that catalyzes GDP/GTP exchange on Arf, the GBF and BIG ArfGEFs have five common homology domains. Very little is known about the functions of these non-catalytic domains, but it is likely that they serve to integrate upstream signals that define the conditions of Arf activation. Here we describe interactions between two conserved domains upstream of the Sec7 domain (DCB and HUS) that determine the architecture of the N-terminal regions of the GBF and BIG ArfGEFs using a combination of biochemical, yeast two-hybrid and cellular assays. Our data demonstrate a strong interaction between DCB domains of GBF1, BIG1 and BIG2 to maintain homodimers, and an interaction between DCB and HUS domains within each homodimer. The DCB/HUS interaction is mediated by the HUS box, the most conserved motif in large ArfGEFs after the Sec7 catalytic domain. In support of the *in vitro* data, we show that both the DCB and the HUS domains are necessary for GBF1 dimerization in mammalian cells, and that the DCB domain is essential for yeast viability. We propose that the dimeric DCB-HUS structural unit exists in all members of the GBF and BIG ArfGEF groups and in the related Mon2p family, and likely serves an important regulatory role in Arf activation.

Small GTP-binding proteins of the Arf family are major regulators of membrane traffic in the exocytotic and endocytic pathways (reviewed in (1)). They are activated by the exchange of GDP for GTP, which is stimulated by guanine nucleotide exchange factors (ArfGEFs) carrying a catalytic Sec7 domain (reviewed in (2,3)). Evidence is accumulating that ArfGEFs integrate upstream signals that define the conditions of Arf activation. First, ArfGEFs localize to specific trafficking organelles (4-9), which allows them to specify which subcellular site requires Arf activity. Second, binding partners involved in cell signaling such as protein kinase A, FK506-binding protein 13 and the AKAP-interacting protein AMY-1 have been identified for the large Golgi-localized ArfGEFs (10 ,11 ,12). Finally, ArfGEFs may play a role in membrane recruitment of Arf effectors such as coats, thus assembling downstream components of Arf signaling pathways prior to Arf activation (5,13).

An essential issue is to decipher how ArfGEFs implement these functions and coordinate them with their biochemical GDP/GTP exchange activity. To address this question, we chose to focus on the large ArfGEFs, as (i) they are the only ArfGEFs found in all eukaryotes and (ii) their multi-domain architecture may allow them to recapitulate the largest number of ArfGEF functions within a single polypeptide (14,15). Large ArfGEFs comprise two groups, to which we refer as the GBF and BIG groups after their names in mammals. Both function in maintaining organelle integrity and membrane traffic at the Golgi or at endosomes (reviewed in (1)). The best studied representatives are yeast Gea1p/Gea2p, *A. thaliana* GNOM and mammalian GBF1 for the

GBF group, and yeast Sec7p and mammalian BIG1/BIG2 for the BIG group (reviewed in (1,2)). We predicted earlier from a bioinformatics analysis that the GBF and BIG groups share a common architecture, suggesting that both ArfGEF groups follow a common scenario for their activation of Arf (15). The predicted organization comprises two non-catalytic domains (DCB and HUS) in the N-terminus of the Sec7 domain, and three in its C-terminus (HDS1, HDS2 and HDS3). The N-terminal DCB (Dimerization and Cyclophilin-Binding) domain (**Figure 1A**) is the only domain to which a molecular function has been assigned. It was originally identified in plant GNOM, where it was shown to be capable of dimerization in yeast two-hybrid and *in vitro* pull-down assays (16). Little is known about the other domains, except for an almost invariant 5-residue motif in the HUS domain, the HUS box (15,17) (Figure 1B), which is essential for aspects of Golgi traffic in yeast (18).

Here we combine biochemical, yeast two-hybrid and cellular assays to analyze the domain architecture and interdomain interactions of the GBF and BIG groups of large ArfGEFs. Our data demonstrate the existence of two distinct interactions involving the DCB domain of the mammalian large ArfGEFs: homodimerization via a DCB/DCB interaction (generalizing previous results from plants), and a novel DCB/HUS interaction depending on the HUS box. We propose that the DCB/DCB and DCB/HUS interactions define a common structure in all members of the BIG and GBF groups of ArfGEFs, which likely also exists in the related eukaryotic Mon2p family.

EXPERIMENTAL PROCEDURES

Expression of recombinant DCB_{BIG1}, DCB_{BIG2} and DCB-HUS-$Sec7_{BIG1}$

The DCB domain of human BIG1 (DCB_{BIG1}, residues 2-224) was introduced into pET28a (Novagen) modified to remove the thrombin cleavage site and to include alternative restriction sites (*Kpn*I and *Age*I). The E221K mutation was introduced into DCB_{BIG1} by PCR using the QuikChange site-directed mutagenesis kit (Stratagene). Both wild type and mutant DCB_{BIG1} were expressed in the *Rosetta*(*DE3*)pLysS *E. coli* strain (Merck KGaA). DCB_{BIG1} was purified on a Ni^{2+}-NTA affinity column (GE-Healthcare) followed by precipitation in ammonium sulphate to 70% saturation and gel filtration on a Superdex 75 column (GE-Healthcare). The DCB domain of human BIG2 (DCB_{BIG2}, residues 2-224) was cloned, expressed and purified as described for DCB_{BIG1}.

A construct spanning the DCB, HUS and Sec7 domains of human BIG1 (DCB-HUS-$Sec7_{BIG1}$, residues 2-888) was introduced into pFastBac HTA vector (Invitrogen) using *Eco*RI and *Kpn*I restriction sites. Sf21 cells infected by baculoviruses harboring this construct were used to express DCB-HUS-$Sec7_{BIG1}$. The recombinant protein was purified on a Ni^{2+}-NTA affinity column followed by a desalting column and a gel filtration Superdex 200 column (GE-Healthcare). Limited proteolysis was performed with 10 units of thrombin (Amersham) per mg of protein at room temperature overnight. DCB-HUS-$Sec7_{BIG1}$ and its proteolysis products were analyzed by SDS-PAGE and Western Blot.

Biophysical assays.

Sedimentation velocity was measured at 40000 *g* for 24 hours and analysed with the *SVEDBERG* software (www.jphilo.mailway.com/svedberg.htm).

Sedimentation equilibrium experiments were carried out at 10 000, 15 000 and 20 000 *g* for 46 hours and analyzed with the Origin software (Beckman Coulter). Circular dichroism (CD) scans were recorded between 185 and 260 nm. Thermal denaturations were carried out in the temperature range of 5 to 95°C at a rate of 2°C/min. Secondary structure composition was estimated with the *CDDSTR* software (19). The effect of protein concentration on its thermal denaturation was measured with 0.3, 0.75 and 3 µM DCB_{BIG1} and analyzed at 222 nm, a wavelength minimum that is characteristic of α-helices.

Yeast two-hybrid assays.

Plasmids expressing human BIG1 and BIG2 and *C. griseus* GBF1 are gifts from P. Melançon (University of Alberta, Canada), the plasmid expressing coxsackievirus 3A is a gift from F. van Kuppeveld (Radboud University Nijmegen Medical Centre, The Netherlands). All yeast two-hybrid constructs were cloned in the pASΔ and pACT2 vectors to create fusions with the Gal4-

DNA binding domain (BD) and Gal4 transcription activation domain (AD) respectively. The Y190 (MATa, *gal4-542*, *gal80-538*, *his3*, *trp1-901*, *ade2-101*, *ura3-52*, *leu2-3, 112*, URA3::GAL1-LacZ, Lys2::GAL1-HIS3cyh^r*)* and AH109 (MATa*, trp1-901, leu2-3, 112, ura3-52, his3-200 gal4*Δ*, gal80*Δ*,* LYS2::GAL1$_{UAS}$-GAL1$_{TATA}$-HIS3, GAL2$_{UAS}$-GAL2$_{TATA}$-ADE2, URA3::MEL1$_{UAS}$-MEL1$_{TATA}$-lacZ) yeast strains were transformed with the different recombinant plasmids using the lithium acetate method (20). Y190 transformants autotrophic for tryptophan and leucine were assayed for β-galactosidase activity using the filter technique (21). AH109 transformants were tested for expression of *HIS3* and *ADE2* reporter genes. Stable expression of each clone in pACT2 and pASΔ was confirmed by Western blot using Santa Cruz's Gal4-AD and Gal4-BD monoclonal antibodies, respectively. All experiments were performed at least 3 times.

Biochemical assays.
Liposome binding experiments were performed with liposomes prepared as described in (22) (Table 1). DCB$_{BIG1}$ (1 μM) was incubated at room temperature in 50 mM Hepes pH 7.2 and 120 mM potassium acetate with sucrose-loaded vesicles (final lipid concentration, 1 mM) in small polycarbonate tubes. The samples were centrifuged at 360 000 *g* for 20 min and the supernatants and the pellets were analyzed by SDS–PAGE with Sypro-orange staining. The Sec7 domain of BIG1 was used as a negative control. Exchange reaction assays were performed by tryptophan fluorescence kinetics using Δ17Arf1 as described in (23). The effect of DCB$_{BIG1}$ on the exchange rate of Sec7$_{BIG1}$ was analyzed by comparing the results of experiments done in the absence or presence of DCB$_{BIG1}$ (10 μM).

Co-immunoprecipitation assays.
COS7 cells in 10 cm culture dishes were cotransfected with the plasmids pHA-GBF1 expressing human HA-GBF1 and either Venus-GBF1, Venus-GBF1Δ889 or YFP-GBF1-C expressing, respectively, human GBF1 and GBF1 deleted of the first 297 (ΔDCB) and 710 amino acids (ΔDCB-HUS) (T.K Niu and C. L. Jackson, unpublished data). After 20 hours of expression, cells were washed two times with 5 mL of cold PBS (137 mM NaCl, 2.7 mM KCl, 19 mM Na_2HPO_4, 1,8 mM KH_2PO_4), then disrupted in 0.5 mL of cold Lysis buffer (50 mM Tris-HCl pH 7.5, 100 mM NaCl, 1 mM EDTA, 1 % NP40). After centrifugation at 4°C, soluble cellular extracts were precleared with 20 μL of protein G Sepharose 4 Fast Flow (GE Healthcare) at 4°C for 30 minutes. Supernatants were incubated with 3 μg of anti-GFP antibodies (Roche) for 1.5 hours at 4°C. Then, 30 μL of protein G Sepharose 4 Fast Flow was added and the mixtures were incubated at 4°C for 1.5 hours. The resin was washed two times with 1 mL of W100 buffer (50 mM Tris-HCl pH 7.5, 100 mM NaCl, 1 mM EDTA) followed by two washes with 1 mL of PBS. Proteins were then eluted by incubation with 60 μL of SDS-PAGE sample buffer for 5 minutes at 95°C. Eluted proteins were separated on a 6% SDS-PAGE gel and analyzed by Western immunoblotting using anti-HA antibodies as primary antibody (Sigma).

Plasmid shuffle assays in yeast
The *gea1*-Δ*DCB* construct (coding for residues 233-1408 of Gea1p) was obtained by introducing a gap in the pAP22 (CEN, *TRP1*, *GEA1*) (gift of A. Peyroche, CEA, Saclay, France). The PCR product extended to 1825 and 154 base pairs past the 5' and 3' ends of the gap, respectively. The mutated fragment and gapped plasmid were used to transform CJY52-10-2 yeast cells that contained the pAP23 plasmid (CEN, *URA3*, *GEA1*) (24). Transformants were plated onto synthetic medium plates lacking tryptophan. Trp+ clones were grown at 30°C in minimal medium (YNB) containing 0.67% yeast nitrogen base without amino acids (BD), supplemented with appropriate nutrients and with 2% glucose. 5-fluoroorotic acid monohydrate (5-FOA, Toronto Research Chemicals) was added to a final concentration of 0.1% to counterselect the *URA3*-containing cells. The presence of protein product of the *gea1*-Δ*DCB* allele was controlled by Western immunobloting as follows. Total yeast cell protein extracts were prepared using the NaOH/trichloroacetic acid lysis technique (25). Proteins were separated by SDS-PAGE in 10% tricine gels and were analyzed by immunoblotting. The primary antibody was either a polyclonal anti-Gea1p antibody or a monoclonal anti-Vat2p antibody directed against a subunit of the vacuolar ATPase (Invitrogen).

Results

Mammalian BIG and GBF ArfGEFs have an N-terminal dimerization DCB domain. Using a bioinformatics approach, we predicted previously that the DCB domain, originally identified as a dimerization domain in the GBF group member GNOM (16), is also present at the N-terminus of large ArfGEFs from the BIG group where it should form an all-helical domain (15). In order to address this question experimentally, we expressed in *E. coli* the N-terminus of human BIG1, encompassing the helical subdomain of highest sequence homology and the more variable N-terminal subdomain (**Figure 1A**), and purified it to homogeneity. The recombinant protein behaved as a 2x26 kDa dimer (**Figure 2A**), a molecular weight that was confirmed by analytical ultracentrifugation (AUC) equilibrium sedimentation (54.3 kDa). A similar construct from human BIG2 was also expressed and purified to homogeneity, and as for BIG1 eluted as a dimer on a gel filtration column (**Figure 2A**). Deconvolution of circular dichroism (CD) spectra for both proteins was consistent with a mostly helical secondary structure. We thus conclude that the N-terminal domain of human BIGs qualifies as the *bona fide* homolog of the DCB domain of the GBF group member GNOM and refer to it as DCB_{BIG} hereafter.

In order to assess a possible dimer/monomer equilibrium, we analyzed the CD thermal denaturation spectra of DCB_{BIG1} (**Figure 2B**). The model providing the best fit for the data was a two-state transition between an all-helical structure and a random coil denaturated state, without formation of a monomeric intermediate. This, and a denaturation temperature (69°C) independent of the protein concentration and higher than the average for proteins (around 55°C), suggest that the dimer is stable with a dissociation constant below the concentration used in the experiment (100 nM). AUC confirmed the predominance of a dimeric species and the absence of monomer.

To determine whether dimerization is a general feature of DCB-like domains of the large ArfGEFs, we tested mammalian GBF1 and BIG2 DCB/DCB interactions using the yeast 2-hybrid system. We observed a strong interaction between DCB domains of hamster GBF1 (98% identity with human GBF1) and between human BIG2 DCB domains, indicating that the DCB domain mediates dimerization in all mammalian large ArfGEFs (**Figure 3, sectors 1 and 12**). We next looked for residues that contribute to the DCB/DCB interaction. Two highly conserved residues, K91 and E130 in DCB_{GBF1}, are found in both large ArfGEF groups (**Figure 1A**). Mutation of either residue to alanine in DCB_{GBF1} abolished the interaction between mutant and wild-type DCB_{GBF1} in the two-hybrid system (**Figure 3, sectors 2 and 11**). Thus, these residues are either part of the dimer interface, or induce an abnormal structure in this interface. We then analyzed a mutation found in the C-terminus of the DCB domain of human BIG2 (**Figure 1A**), which has been associated with a congenital disease, autosomal recessive periventricular heterotopia with microencephaly (ARPHM; (26)). DCB_{BIG1} carrying the equivalent mutation, E221K, was expressed in *E. coli* with a solubility similar to that of wild-type DCB_{BIG1}. AUC experiments showed that DCB_{BIG1}^{E221K} forms a dimer (data not shown). Thus, functions of DCB_{BIG2} other than dimerization are affected by this mutation in the ARPHM disorder.

A novel interaction between the DCB and HUS domains in large ArfGEFs. To determine whether interactions exist between the different domains of the large ArfGEFs, we carried out an extensive yeast two-hybrid analysis of domain-domain interactions for mammalian GBF1 and BIG1. All five non-catalytic domains in addition to the catalytic Sec7 domain were considered. For GBF1 (**Table 2A**) and BIG1 (**Table 2B**), only one interaction was detected in addition to the DCB/DCB interaction described above. In both cases, a strong interaction between the DCB and HUS domains of each ArfGEF was observed (**Figure 3, sectors 3 and 4).** This interaction was independent of the variable DCB-HUS linker added on either the DCB or HUS side (**Table 2A**). A strong interaction was also found between the DCB and HUS domains of human BIG2 (**Figure 3, sector 5**).

The HUS box is an almost invariant N(Y/F)DC(D/N) motif, which is predicted to lie between two α-helices (**Figure 1B**). Mutation of the central aspartate to alanine in this motif abolished the DCB/HUS interaction in both GBF1

and BIG1 (**Figure 3, sectors 18 and 19**). Thus, the HUS box supports the DCB/HUS interaction, which is the first molecular function to be associated with this motif. We then analyzed whether mutations that impair the DCB/DCB interaction (see above) also affect the DCB/HUS interaction. The E130A mutation in GBF1, but not the K91A mutation, abolished the DCB/HUS interaction (**Figure 3, sectors 16 and 17**). These results indicate that residue K91 is involved only in the DCB/DCB interaction, whereas the E130 residue is involved in both interactions.

Next, we used the yeast two-hybrid system to analyze DCB/DCB and DCB/HUS interactions within GBF1 constructs spanning more than one domain. We first analyzed the ability of the DCB domain alone to interact with larger ArfGEF fragments. DCB_{GBF1} interacted with DCB-HUS_{GBF1}, DCB-HUS-$Sec7_{GBF1}$ and with full-length GBF1 (**Figure 3, sectors 7, 8 and 10**). Although these yeast two-hybrid interactions appeared to be weaker than the interaction between two DCB domains alone, they strongly suggest that the DCB/DCB interaction occurs also in the context of the full-length GBF1 protein. We then analyzed the DCB/HUS interaction in the context of multiple domains. A strong interaction was found between the DCB domain and a HUS-Sec7 construct (**Figure 3, sector 6**). HUS_{GBF1} also interacted with DCB-HUS-$Sec7_{GBF1}$ and full-length GBF1, although more weakly than with DCB_{GBF1} alone (**Figure 3, sectors 14 and 15**). In support for the dimerization of the N-terminal region taking place in larger constructs, recombinant DCB-HUS-$Sec7_{BIG1}$ eluted on a gel filtration column with a molecular weight consistent with a dimer (**Figure 2A**).

No interactions between the non-catalytic domains other than the DCB/DCB and DCB/HUS interactions were identified with the yeast two-hybrid assay. We also failed to detect an interaction of the non-catalytic domains with the Arf1 substrate (data not shown). In addition, we did not observe any DCB/DCB or DCB/HUS cross interactions between BIG1, BIG2 and GBF1 in the yeast two-hybrid system (data not shown),

Functions of DCB/DCB and DCB/HUS interactions in ArfGEF dimers.

The DCB domain has features of a dimeric helical bundle, which is a frequent arrangement in cytosolic proteins involved in membrane recruitment, such as the membrane curvature-sensing BAR domain found in amphiphysins and Arfaptin/POR, an Arf effector (27). We thus investigated the binding of DCB_{BIG1} to liposomes of various compositions using a sedimentation assay (**Table 1, Figure 4A**). However, no such interaction could be observed regardless of the liposome composition, suggesting that the DCB homodimer does not have membrane-binding properties on its own.

The Sec7 domain did not interact with the constructs tested in our yeast two hybrid analysis (**Tables 2A and 2B; Figure 3, sectors 9 and 20**). To further analyze whether the N-terminus could regulate the catalytic exchange activity of the Sec7 domain, we used recombinant proteins and a fluorescence kinetics assay. We first analyzed the effect of excess DCB_{BIG1} on the exchange rate of the Sec7 domain of human BIG1 ($Sec7_{BIG1}$) using Δ17Arf1 as substrate. No inhibition or stimulation of the exchange rate by DCB_{BIG1} could be observed, regardless of whether Δ17Arf1, $Sec7_{BIG1}$ or both had been pre-incubated with DCB_{BIG1} (**Figure 4B**). We then analyzed the catalytic activity of a BIG1 construct spanning the DCB-HUS-Sec7 domains using the same fluorescence assay. This construct was active at stimulating GDP/GTP exchange on Δ17Arf1 (**Figure 4C**) and it was inhibited by BFA with a Ki of 23.9±7.2 μM which is similar to that measured for the Sec7 of BIG1 alone (23). To confirm that the DCB-HUS tandem had no effect on the catalytic activity, we took advantage of a unique thrombin cleavage site located at residue 622 between the HUS and Sec7 domains, which allowed us to generate free DCB-HUS_{BIG1} and $Sec7_{BIG1}$ by limited proteolysis. Exchange rates measured with a BIG1 peptide concentration of 0.5 μM were in the same range for the uncleaved and cleaved fragments (0.073 ± 0.005 s^{-1} and 0.098 ± 0.012 s^{-1}, respectively), suggesting that the DCB-HUS tandem does not have a simple one-to-one regulatory activity towards the Sec7 domain.

The N-terminus of large ArfGEFs interacts with several large ArfGEF protein partners (reviewed in (1)). We thus investigated whether the DCB/HUS structure may be required for protein-protein interactions. To this end, we took advantage of the fact that the N-terminus of GBF1 binds to 3A, a protein from enteroviruses that blocks host cell

secretion by inhibiting GBF1 function (28). The cytosolic portion of 3A (residues 1-60) interacts with DCB-HUS$_{GBF1}$ and DCB-HUS-SEC7$_{GBF1}$ in the yeast two-hybrid assay (**Figure 3, sector 21**). In contrast, no interaction was observed with individual DCB or HUS domains (**Figure 3, sectors 22 and 23**). This is consistent with data showing that deletion of either the first 50 amino acids of GBF1 or deletion of the HUS domain and downstream sequences abolishes interaction with the 3A protein in the mammalian two-hybrid system (29). These results show that portions of both the DCB and HUS domains of GBF1 are required for binding to the viral 3A protein, and suggest the possibility that an integral DCB-HUS structure is necessary for binding of the 3A protein.

Dimerization of large ArfGEFs in vivo. The above analysis suggests that the DCB domain supports the dimerization of large ArfGEFs and organizes a structure that can bind protein partners. We thus assessed the dimerization and function of this domain in cells for two large ArfGEFs of the GBF group.

We first analyzed the formation of human GBF1 dimers in mammalian cells by pull-down assays (**Figure 5A**). We found out that full-length GBF1 can easily be isolated as a dimer from mammalian cells. Next, we examined dimer formation between the full-length GBF1 and forms of GBF1 deleted of the DCB domain alone or of both the DCB and HUS domains. Clearly, whereas deletion of the DCB domain alone reduced somewhat the formation of a dimer with full-length GBF1, both the DCB and HUS domains had to be deleted to nearly abolish dimer formation. Thus, the DCB and the HUS domains are both involved in the dimerization of GBF1.

We then analyzed the effect of deleting the DCB domain of Gea1p, a member of the GBF group of large ArfGEFs in yeast, using a plasmid shuffle strategy. The strain used contains the wild-type *GEA1* gene on a *URA3* plasmid with both *gea1*Δ and *gea2*Δ deletions of the chromosomal copies of the genes (24). The *gea1*-Δ*DCB*- allele was introduced into a low-copy *TRP* plasmid. The Gea1p-ΔDCB protein was expressed and was not degraded (**Figure 5B**). Clones failed to grow at 30°C upon the loss of the wild-type *GEA1* plasmid when the *gea1*-Δ*DCB* plasmid became the sole copy of the redundant *GEA1* and *GEA2* genes (**Figure 5C**). This result indicates that the DCB domain of Gea1p is essential for yeast viability.

DISCUSSION

A conserved DCB/DCB and DCB/HUS structure in eukaryotic large ArfGEFs and the related Mon2p family. In this study, we investigated the domain-domain interactions within the BIG and GBF groups of large ArfGEFs, which we predicted previously to share a common architecture (15). Based on biochemical and yeast two-hybrid analyses of mammalian BIG1, BIG2 and GBF1, we establish that all three members share a similar DCB-HUS organization upstream of their Sec7 domains, in which the DCB domain interacts with itself and with the HUS domain. The DCB/HUS interaction requires the highly-conserved HUS box, a five amino acid motif found in all members of the BIG and GBF groups of ArfGEFs.

Because of its bipartite organization, the DCB-HUS tandem provides different ways for large ArfGEFs to form multimers. One is through the DCB/DCB interaction, which is an obligate intermolecular interaction. Since the DCB domain forms a strong homodimer *in vitro*, we propose that it supports constitutive homodimerization of large ArfGEFs. The existence of this interaction in native BIG and GBF ArfGEFs is supported by its formation in a range of yeast two-hybrid GBF1 constructs, the dimerization of the recombinant BIG1 and BIG2 constructs and our *in vivo* data on GBF1. It is also consistent with the molecular weight of several large ArfGEFs of both the BIG and GBF groups as measured by size exclusion chromatography, including yeast Gea1p (30), human BIG1 and BIG2 (31 ,32) and plant GNOM (16). All elute as large molecular weight complexes, which, given the uncertainty of this technique for non-globular proteins, is consistent with their association as homodimers.

In contrast, the DCB/HUS interaction can occur either between two monomers (intermolecular) (**Figure 6A**) or within a single ArfGEF polypeptide (intramolecular) (**Figure 6B**). An intermolecular DCB/HUS interaction would provide a second contribution to dimerization in addition to the DCB/DCB interaction. This possibility is supported by our co-

immunoprecipitation results, which show that the ΔDCB form of human GBF1 formed a dimer with full-length GBF1 almost as efficiently as full-length GBF1 in mammalian cells, whereas deletion of both DCB and HUS domains practically eliminated dimerization with full-length GBF1. Interestingly, the HUS box has an unusual level of sequence conservation and content of polar residues within a protein interface, pointing to a potential for the DCB/HUS interaction to open up and expose the HUS box (**Figure 6C**). The HUS box could then carry out other functions, allowing in particular the formation of ArfGEF tetramers through three-dimensional (3D) domain swapping (**Figure 6D**). An interesting corollary is that this could allow large ArfGEFs to form heterotetramers, which are more likely to form than heterodimers given the stability of the homodimeric DCB/DCB interaction. BIG1 and BIG2 have been shown to co-immunoprecipitate in human cells (32), which could thus be mediated by the formation of heterotetramers containing one BIG1 homodimer and one BIG2 homodimer

A region homologous to the DCB and HUS domains is present in a novel eukaryotic protein family, Mon2p/Ysl1p/SF21, that is related to the large ArfGEFs (33-35) but lacks the Sec7 nucleotide exchange domain (34,35). Yeast Mon2p has been shown to localize to late Golgi/endosomes (33-35) and to bind Arl1p (33), a close relative of Arf proteins. We propose that members of the Mon2p family feature a DCB-HUS structure, including a DCB homodimerization domain (**Figure 1A**) and a HUS domain with a candidate HUS box containing the central (Y/F)D motif (**Figure 1C**) and capable of forming a DCB/HUS interaction. DCB/DCB-mediated dimerization is in agreement with the co-immunoprecipitation of yeast Mon2p as a homodimer (34). The presence of the DCB-HUS module without an associated Sec7 domain in these proteins is consistent with a structural function that is independent of the biochemical nucleotide exchange activity.

The role of the DCB-HUS structure in large ArfGEF interactions. The N-terminus of large Golgi ArfGEFs has been reported to interact with various protein partners. Notably, the N-terminus of GBF1 interacts with Rab1 (36) and regions of mammalian BIGs encompassing DCB-HUS interact with AMY-1 (12) PKA (10), FKBP13 (11), the Exo70 subunit of the exocyst (37) and the HSC70 chaperone (12). The requirement of 3A protein for both the DCB and HUS domains suggests that the two-domain DCB-HUS structure could mediate these protein-protein interactions in addition to its dimerization function. Furthermore, phenotypic data *in vivo* have shown that the DCB-HUS tandem is necessary and sufficient to define the subcellular localization of p200/BIG1 to Golgi membranes (17,18). Interestingly, this is also the case for the DCB-HUS homology region of the related protein Mon2p (34). Furthermore, mutation of the HUS box in Gea2p in yeast, which is likely to disrupt the DCB/HUS interface according to our study, resulted in impaired membrane association together with a severe defect of anterograde ER/Golgi traffic (18). Thus, the DCB-HUS structure is likely to contribute to large ArfGEF functions upstream of their exchange activity, including interactions that define their localization. Further investigations are now needed to establish whether the DCB/HUS interaction is constitutive, or supports a regulated switch between a closed and an open conformation capable of alternative interactions. The DCB/HUS structure characterized here should provide a rational framework to address this issue in the BIG and GBF groups of ArfGEFS.

FOOTNOTES

ACKNOWLEDGEMENTS:

This work was supported by a Human Frontiers in Science Program grant and a French Ministère de la Recherche ACI grant to J.C. and a CNRS ATIP grant to V.B.. P.S. was supported by a grant from the CNRS ; C. O.-S. by a Marie-Curie grant from the European Community. We thank Barbara Mouratou (LEBS, CNRS, Gif-sur-Yvette, France) for initiating the yeast two hybrid analysis, and Julie Leroux (LEBS, CNRS, Gif-sur-Yvette, France) for excellent technical assistance with the yeast two hybrid assays; Fatima el Khadali (LEBS, CNRS, Gif-sur-Yvette, France) for performing the AUC experiments; Simona Burlacu-Miron and Gil Craescu (CNRS/Institut Curie, Orsay, France) for their help with circular dichroism; Bruno Antonny (IPMC, CNRS, Valbonne, France) for his help with the liposome assay ; Sylvie Lazareg and Jean-Pierre le Caer (ICSN, CNRS, Gif-sur-Yvette, France) for performing mass spectrometry measurements ; and Rosine Haguenauer-Tsapis (Institut Jacques Monod-CNRS, Paris, France) for her support.

Abbreviations list:

Arf, **ADP-ribosylation factor**
ArfGEF, **guanine nucleotide exchange factors of Arf proteins**
GBF1, **Golgi-associated BFA-resistant guanine nucleotide exchange Factor**
BIG, **BFA-Inhibited Guanine nucleotide exchange factor**
DCB**, Dimerization/Cyclophilin Binding**
HUS**, Homology Upstream of Sec7**
HDS**, Homology Downstream of Sec7**
GTP, **Guanosine triphosphate**
GDP, **Guanosine diphosphate**
5-FOA**, 5-fluoroorotic acid**
BFA**, Brefeldin A**

FIGURE LEGENDS

Figure 1. Sequence alignments of DCB domains and HUS boxes.

A, Sequence alignment of DCB domains of the BIG, GBF and Mon2p/Ysl1p/SF21 families. Predicted α-helices are represented by helices. Black arrows indicate the conserved residues mutated in *C. griseus* GBF1. The grey arrow indicates the BIG2 glutamate mutated in ARPHM and analyzed in this paper.

B, Sequence alignment of the HUS box (framed) in the HUS domain. The mutation analyzed in this study is shown by an arrow.
C. Sequence alignment of the putative HUS box (framed) in the eukaryotic Mon2p/Ysl1p/SF21 family. The residue shown by an arrow is equivalent to that in Figure 1B.

Figure 2. Biochemical characterization of recombinant proteins

A, Elution profiles of purified DCB_{BIG1}, DCB_{BIG2}, DCB-HUS-$Sec7_{BIG1}$ on a gel filtration column. The elution volumes of calibration proteins are indicated.

B, Circular dichroism spectra of DCB_{BIG1} (6 μM) as a function of temperature. CD spectra are taken every 5 degrees. The isodichroic point lies at 200.5 nm (thin arrow), showing that unfolding occurs as a two-state helix-coil transition.

Figure 3. Yeast two-hybrid analysis of DCB and HUS interactions in mammalian ArfGEFs.

AH109 yeast cells were co-transformed with the expression plasmids for bait (BD) and prey (AD) fusion proteins and selected on double synthetic dropout (–Trp/–Leu) medium plates. The transformants were then selected for the expression of *HIS3* and *ADE2* genes, by growing on synthetic dropout medium (-Trp/-Leu/-His/-Ade).
1: DCB_{GBF1}/DCB_{GBF1}; 2: DCB_{GBF1}/DCB_{GBF1}^{K91A}; 3: DCB_{GBF1}/HUS_{GBF1}; 4: DCB_{BIG1}/HUS_{BIG1};
5: DCB_{BIG2}/HUS_{BIG2}; 6: DCB_{GBF1}/HUS-$Sec7_{GBF1}$; 7: DCB_{GBF1}/DCB-HUS_{GBF1};
8: DCB_{GBF1}/DCB-HUS-$Sec7_{GBF1}$; 9: DCB_{GBF1}/$Sec7_{GBF1}$; 10: DCB_{GBF1}/GBF1;
11: DCB_{GBF1}-DCB_{GBF1}^{E130A} ; 12: DCB_{BIG2}/DCB_{BIG2} ; 13: GBF1/DCB-HUS-$Sec7_{GBF1}$;
14: HUS_{GBF1}/DCB-HUS-$Sec7_{GBF1}$; 15: HUS_{GBF1}/GBF1 ; 16: HUS_{GBF1}/DCB_{GBF1}^{K91A} ;
17: HUS_{GBF1}/DCB_{GBF1}^{E130A} ; 18: HUS_{GBF1}^{D540A}/DCB_{GBF1}; 19: HUS_{BIG1}^{D570A}/DCB_{BIG1};
20:HUS_{GBF1}/$Sec7_{GBF1}$; 21: DCB-HUS_{GBF1}/3A ; 22: HUS_{GBF1}/3A ; 23: DCB_{GBF1}/3A

Figure 4. Function of the DCB/DCB and DCB/HUS interactions.

A, Sedimentation analysis of DCB_{BIG1} binding properties to liposomes. The lanes correspond (in this order) to molecular weight markers, supernatant (S) and pellet (P) fractions of experiments with no liposomes (No lip) and liposomes 1 to 4 (Table 1). The last lane represents the total amount of protein in the experiment (T).

B, Effect of DCB_{BIG1} on the kinetics of $Sec7_{BIG1}$-stimulated GDP/GTP exchange on Δ17Arf1 measured by tryptophan fluorescence. 1, no DCB; 2, DCB_{BIG1} was incubated with Sec7 domain for 5 mn before Δ17Arf1-GDP was added; 3, DCB_{BIG1} was incubated with Arf1 for 5 mn before the Sec7 domain was added. In all cases, GTP (100 μM) was added 2 mn after all proteins were mixed together.

C, GDP/GTP exchange activity of DCB-HUS-$Sec7_{BIG1}$ on Δ17Arf1 measured at different GEF concentrations.

Figure 5. *In vivo* assays

A, The DCB and HUS domains of human GBF1 are both involved in its dimerization in mammalian cells. HA-tagged GBF1 was coexpressed with either GFP, GFP-tagged GBF1, GFP-tagged GBF1ΔDCB or GFP-tagged GBF1Δ(DCB-HUS). After incubation with anti-GFP antibodies followed by an incubation with protein G Sepharose, the resin was washed several times and proteins eluted by incubation with SDS-PAGE sample buffer. Eluted proteins were separated on a 6% SDS-PAGE gel and analyzed by Western blotting using anti-HA antibodies

B, Yeast extracts from Δ*gea1*Δ*gea2* cells bearing a *URA3* plasmid containing the *GEA1* wild type gene (plasmid pAP23, lane 1), or pAP23 and a *TRP* plasmid containing the *GEA1* wild-type gene (pAP22, lane 2), or pAP23 and pAP22 containing the *gea1*-Δ*DCB1* gene (lane 3) or yeast extracts from a wild-type strain (lane 4) were separated on SDS polyacrylamide gels and analyzed by western immunoblotting using an anti-Gea1p antibody. An anti-Vat2p antibody was used as a loading control.

C, Yeast cells deleted for the *GEA1* and *GEA2* genes and bearing a *URA3* plasmid containing the *GEA1* wild-type gene were transformed with a plasmid containing either the wild type *GEA1* gene (Δ*gea2 GEA1* cells) or the *GEA1* gene deleted for the DCB domain (Δ*gea2 gea1*-Δ*DCB* cells). 10-fold serial dilutions of yeast cultures were plated on media with or without 5-FOA to counterselect the *URA3*-containing cells.

Figure 6. Models for the DCB/DCB and DCB/HUS interactions.

A, Dimerization by combined DCB/DCB and DCB/HUS intermolecular interactions.

B, DCB/DCB dimerization with intramolecular DCB/HUS interaction.

C, A possible regulatory switch of the HUS box from domain/domain interaction to solvent exposure and/or alternative interactions.

D, Tetramer formation by 3D domain swapping.

TABLE LEGENDS

Table 1. Liposome composition (mol %). PC: phosphatidylcholine; PG: phosphatidylglycerol; PIP2: phosphatidylinositol-4,5-bisphosphate. In all cases, 0.2% of the fluorescent lipid nitrobenzoxadizoldihexadecanoyl-phosphatidylethanolamine (NBD-PE) was added as a tracer.

Table 2. Summary of domain/domain interactions in mammalian ArfGEFs analyzed with the yeast two-hybrid assay. Strong interactions are indicated in dark grey, weaker interactions in grey. Baits (BD) and preys (AD) are indicated in lines and columns respectively.

A, Domain interactions in GBF1. Domain limits are: DCB : 1-202 ; DCB-Linker : 1-386 ; HUS : 391-565 ; Linker-Hus : 202-603 ; Linker: 202-386; DCB-HUS: 1-565 ; Sec7 : 682-888 or 696-888 ; HUS-Sec7 : 387-888 ; DCB-HUS-Sec7 : 1-888 ; HDS1 : 889-1059 ; HDS1-HDS2 : 911-1273 ; HDS3 : 1525-1856 ; HDS1-HDS2-HDS3 : 889-1856.

B, Domain interactions in BIG1. Domains limits are: DCB : 2-224 ; HUS : 411-699 ; DCB-HUS : 2-699 ; Sec7 : 411-887 ; HDS1 : 889-1070 ; HDS1-HDS2 : 888-1302 ; HDS3 : 1030-1859.

Table 1

	1	2	3	4
Soybean PC	**95**	**65**	**92.5**	**62.5**
Cholesterol	**5**	**5**	**5**	**5**
Egg PG	**0**	**30**	**0**	**30**
Brain PIP2	**0**	**0**	**2.5**	**2.5**

Table 2:

A

	DCB	DCB-Linker	DCB^{E130A}	HUS	HUS^{D541A}	Linker-HUS	HUS-Sec7	Linker	Sec7	DCB-HUS-Sec7	HDS1	HDS1-HDS2	HDS3
GBF1 (full-length)	+		-	+		+	-	-	-	+			
DCB	+	-	-	+	-	+	+	-	-	+	-	-	-
DCB^{K91A}	-		-	+	-	+	+						
HUS	+	+	-	-		-		-	-	+	-	-	-
Linker-HUS	+		-	-		-			-	+	-	-	
DCB-HUS	+	-	-	-		-			-	+			
Linker	-			-		-		-					
Sec7	-			-		-	-	-	-	-	-	-	-
HUS-Sec7	+			-		-			-	-			
DCB-HUS-Sec7	+		-	-		-	-		-	+		-	
HDS1	-					-			-		-		-
HDS1-HDS2	-			-					-		-	-	-
HDS3	-			-		-			-	-	-	-	-
HDS1-HDS2-HDS3	-			-					-		-	-	-

B

	DCB	HUS	HUS^{D570A}	DCB-HUS	Sec7	HDS1	HDS1-HDS2	HDS3	HDS1-HDS2-HDS3
DCB	-	+	-	-	-	-	-	-	-
HUS	+	-	-	-	-	-	-	-	-
DCB-HUS	-	-	-	-	-	-	-	-	-
Sec7	-	-		-	-	-	-	-	-
HDS1	-	-		-	-	-	-	-	-
HDS1-HDS2	-	-		-	-	-	-	-	-
HDS3	-	-		-	-	-	-	-	-
HDS1-HDS2-HDS3	-	-		-	-	-	-	-	-

REFERENCES

1. D'Souza-Schorey, C., and Chavrier, P. (2006) ARF proteins: roles in membrane traffic and beyond. *Nat Rev Mol Cell Biol* 7(5), 347-358
2. Jackson, C. L., and Casanova, J. E. (2000) Turning on ARF: the Sec7 family of guanine-nucleotide-exchange factors. *Trends Cell Biol* 10. 10(2. 2), 60-67, 60-67.
3. Shin, H. W., and Nakayama, K. (2004) Guanine nucleotide-exchange factors for arf GTPases: their diverse functions in membrane traffic. *J Biochem (Tokyo)* 136(6), 761-767
4. Zhao, X., Lasell, T. K., and Melancon, P. (2002) Localization of large ADP-ribosylation factor-guanine nucleotide exchange factors to different Golgi compartments: evidence for distinct functions in protein traffic. *Mol Biol Cell* 13(1), 119-133
5. Shinotsuka, C., Waguri, S., Wakasugi, M., Uchiyama, Y., and Nakayama, K. (2002) Dominant-negative mutant of BIG2, an ARF-guanine nucleotide exchange factor, specifically affects membrane trafficking from the trans-Golgi network through inhibiting membrane association of AP-1 and GGA coat proteins. *Biochem Biophys Res Commun* 294(2), 254-260
6. Garcia-Mata, R., Szul, T., Alvarez, C., and Sztul, E. (2003) ADP-ribosylation factor/COPI-dependent events at the endoplasmic reticulum-Golgi interface are regulated by the guanine nucleotide exchange factor GBF1. *Mol Biol Cell* 14(6), 2250-2261
7. Geldner, N., Anders, N., Wolters, H., Keicher, J., Kornberger, W., Muller, P., Delbarre, A., Ueda, T., Nakano, A., and Jurgens, G. (2003) The Arabidopsis GNOM ARF-GEF mediates endosomal recycling, auxin transport, and auxin-dependent plant growth. *Cell* 112(2), 219-230
8. Niu, T. K., Pfeifer, A. C., Lippincott-Schwartz, J., and Jackson, C. L. (2004) Dynamics of GBF1, a Brefeldin A-sensitive Arf1 Exchange Factor at the Golgi. *Mol Biol Cell*
9. Shin, H. W., Morinaga, N., Noda, M., and Nakayama, K. (2004) BIG2, a guanine nucleotide exchange factor for ADP-ribosylation factors: its localization to recycling endosomes and implication in the endosome integrity. *Mol Biol Cell* 15(12), 5283-5294
10. Li, H., Adamik, R., Pacheco-Rodriguez, G., Moss, J., and Vaughan, M. (2003) Protein kinase A-anchoring (AKAP) domains in brefeldin A-inhibited guanine nucleotide-exchange protein 2 (BIG2). *Proc Natl Acad Sci U S A* 100(4), 1627-1632
11. Padilla, P. I., Chang, M. J., Pacheco-Rodriguez, G., Adamik, R., Moss, J., and Vaughan, M. (2003) Interaction of FK506-binding protein 13 with brefeldin A-inhibited guanine nucleotide-exchange protein 1 (BIG1): effects of FK506. *Proc Natl Acad Sci U S A* 100(5), 2322-2327
12. Ishizaki, R., Shin, H. W., Iguchi-Ariga, S. M., Ariga, H., and Nakayama, K. (2006) AMY-1 (associate of Myc-1) localization to the trans-Golgi network through interacting with BIG2, a guanine-nucleotide exchange factor for ADP-ribosylation factors. *Genes Cells* 11(8), 949-959
13. Kawamoto, K., Yoshida, Y., Tamaki, H., Torii, S., Shinotsuka, C., Yamashina, S., and Nakayama, K. (2002) GBF1, a guanine nucleotide exchange factor for ADP-ribosylation factors, is localized to the cis-Golgi and involved in membrane association of the COPI coat. *Traffic* 3(7), 483-495
14. Cox, R., Mason-Gamer, R. J., Jackson, C. L., and Segev, N. (2004) Phylogenetic analysis of Sec7-domain-containing Arf nucleotide exchangers. *Mol Biol Cell* 15(4), 1487-1505
15. Mouratou, B., Biou, V., Joubert, A., Cohen, J., Shields, D. J., Geldner, N., Jurgens, G., Melancon, P., and Cherfils, J. (2005) The domain architecture of large guanine nucleotide exchange factors for the small GTP-binding protein Arf. *BMC Genomics* 6(1), 20
16. Grebe, M., Gadea, J., Steinmann, T., Kientz, M., Rahfeld, J. U., Salchert, K., Koncz, C., and Jurgens, G. (2000) A conserved domain of the arabidopsis GNOM protein mediates subunit interaction and cyclophilin 5 binding. *Plant Cell* 12. 12(3. 3), 343-356, 343-356.

17. Mansour, S. J., Skaug, J., Zhao, X. H., Giordano, J., Scherer, S. W., and Melancon, P. (1999) p200 ARF-GEP1: a Golgi-localized guanine nucleotide exchange protein whose Sec7 domain is targeted by the drug brefeldin A. *Proc Natl Acad Sci U S A* 96(14), 7968-7973.
18. Park, S. K., Hartnell, L. M., and Jackson, C. L. (2005) Mutations in a highly conserved region of the Arf1p activator GEA2 block anterograde Golgi transport but not COPI recruitment to membranes. *Mol Biol Cell* 16(8), 3786-3799
19. Whitmore, L., and Wallace, B. A. (2004) DICHROWEB, an online server for protein secondary structure analyses from circular dichroism spectroscopic data. *Nucleic Acids Res* 32(Web Server issue), W668-673
20. Gietz, D., St Jean, A., Woods, R. A., and Schiestl, R. H. (1992) Improved method for high efficiency transformation of intact yeast cells. *Nucleic Acids Res* 20(6), 1425
21. Schneider, S., Buchert, M., and Hovens, C. M. (1996) An in vitro assay of beta-galactosidase from yeast. *Biotechniques* 20(6), 960-962
22. Bigay, J., Gounon, P., Robineau, S., and Antonny, B. (2003) Lipid packing sensed by ArfGAP1 couples COPI coat disassembly to membrane bilayer curvature. *Nature* 426(6966), 563-566
23. Zeeh, J. C., Zeghouf, M., Grauffel, C., Guibert, B., Martin, E., Dejaegere, A., and Cherfils, J. (2006) Dual specificity of the interfacial inhibitor brefeldin a for arf proteins and sec7 domains. *J Biol Chem* 281(17), 11805-11814
24. Peyroche, A., Courbeyrette, R., Rambourg, A., and Jackson, C. L. (2001) The ARF exchange factors Gea1p and Gea2p regulate Golgi structure and function in yeast. *J Cell Sci* 114(Pt 12), 2241-2253
25. Volland, C., Urban-Grimal, D., Geraud, G., and Haguenauer-Tsapis, R. (1994) Endocytosis and degradation of the yeast uracil permease under adverse conditions. *J Biol Chem* 269(13), 9833-9841
26. Sheen, V. L., Ganesh, V. S., Topcu, M., Sebire, G., Bodell, A., Hill, R. S., Grant, P. E., Shugart, Y. Y., Imitola, J., Khoury, S. J., Guerrini, R., and Walsh, C. A. (2004) Mutations in ARFGEF2 implicate vesicle trafficking in neural progenitor proliferation and migration in the human cerebral cortex. *Nat Genet* 36(1), 69-76
27. Peter, B. J., Kent, H. M., Mills, I. G., Vallis, Y., Butler, P. J., Evans, P. R., and McMahon, H. T. (2004) BAR domains as sensors of membrane curvature: the amphiphysin BAR structure. *Science* 303(5657), 495-499
28. Wessels, E., Duijsings, D., Niu, T. K., Neumann, S., Oorschot, V. M., de Lange, F., Lanke, K. H., Klumperman, J., Henke, A., Jackson, C. L., Melchers, W. J., and van Kuppeveld, F. J. (2006) A viral protein that blocks Arf1-mediated COP-I assembly by inhibiting the guanine nucleotide exchange factor GBF1. *Dev Cell* 11(2), 191-201
29. Wessels, E., Duijsings, D., Lanke, K. H., Melchers, W. J., Jackson, C. L., and van Kuppeveld, F. J. (2007) Molecular determinants of the interaction between coxsackievirus protein 3A and guanine nucleotide exchange factor GBF1. *J Virol* 81(10), 5238-5245
30. Peyroche, A., Paris, S., and Jackson, C. L. (1996) Nucleotide exchange on ARF mediated by yeast Gea1 protein. *Nature* 384(6608), 479-481
31. Morinaga, N., Tsai, S. C., Moss, J., and Vaughan, M. (1996) Isolation of a brefeldin A-inhibited guanine nucleotide-exchange protein for ADP ribosylation factor (ARF) 1 and ARF3 that contains a Sec7-like domain. *Proc Natl Acad Sci U S A* 93(23), 12856-12860
32. Yamaji, R., Adamik, R., Takeda, K., Togawa, A., Pacheco-Rodriguez, G., Ferrans, V. J., Moss, J., and Vaughan, M. (2000) Identification and localization of two brefeldin A-inhibited guanine nucleotide-exchange proteins for ADP-ribosylation factors in a macromolecular complex. *Proc Natl Acad Sci U S A* 97(6), 2567-2572
33. Jochum, A., Jackson, D., Schwarz, H., Pipkorn, R., and Singer-Kruger, B. (2002) Yeast Ysl2p, homologous to Sec7 domain guanine nucleotide exchange factors, functions in endocytosis and maintenance of vacuole integrity and interacts with the Arf-Like small GTPase Arl1p. *Mol Cell Biol* 22(13), 4914-4928

34. Efe, J. A., Plattner, F., Hulo, N., Kressler, D., Emr, S. D., and Deloche, O. (2005) Yeast Mon2p is a highly conserved protein that functions in the cytoplasm-to-vacuole transport pathway and is required for Golgi homeostasis. *J Cell Sci* 118(Pt 20), 4751-4764
35. Gillingham, A. K., Whyte, J. R., Panic, B., and Munro, S. (2006) Mon2, a relative of large Arf exchange factors, recruits Dop1 to the Golgi apparatus. *J Biol Chem* 281(4), 2273-2280
36. Monetta, P., Slavin, I., Romero, N., and Alvarez, C. (2007) Rab1b Interacts with GBF1, Modulates both ARF1 Dynamics and COPI Association. *Mol Biol Cell*
37. Xu, K. F., Shen, X., Li, H., Pacheco-Rodriguez, G., Moss, J., and Vaughan, M. (2005) Interaction of BIG2, a brefeldin A-inhibited guanine nucleotide-exchange protein, with exocyst protein Exo70. *Proc Natl Acad Sci U S A* 102(8), 2784-2789

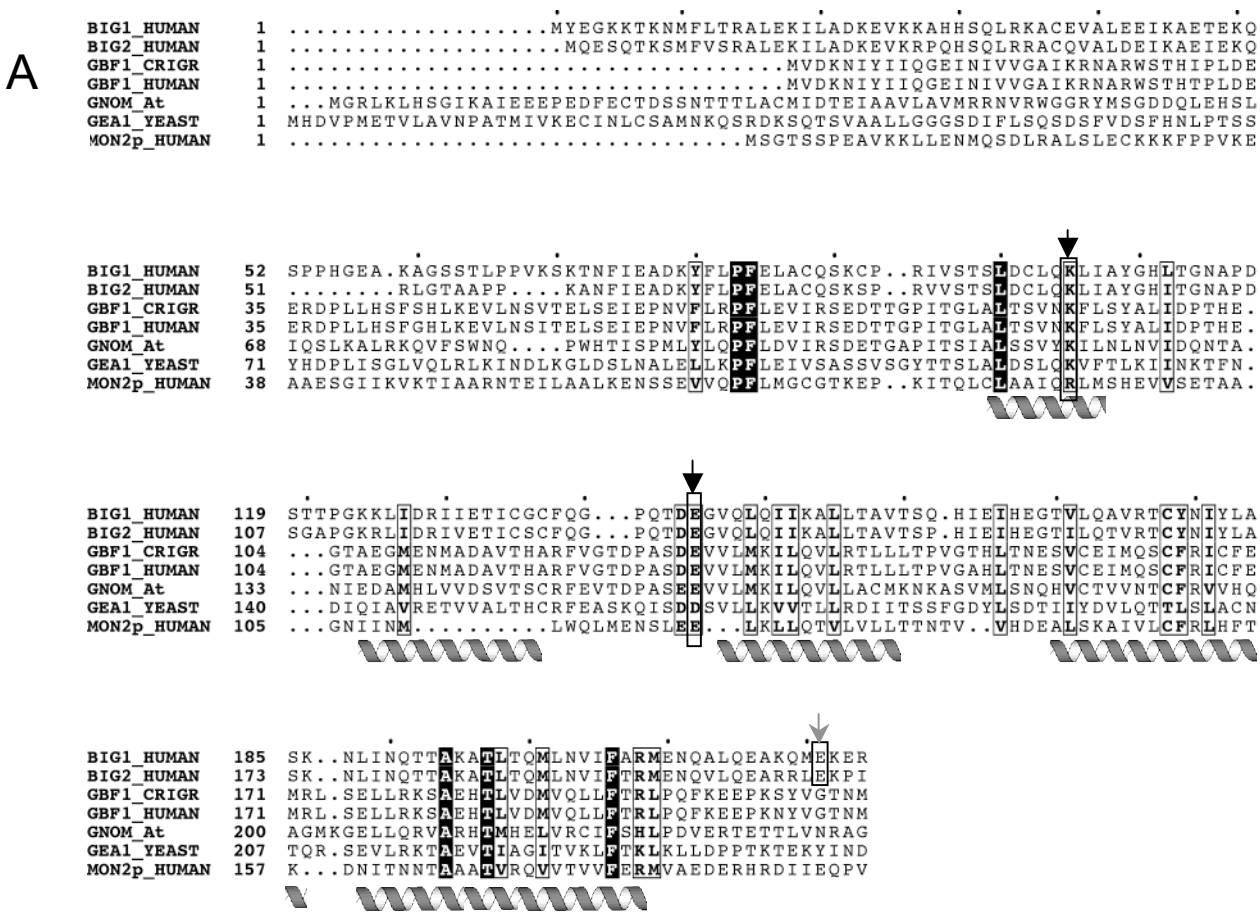
A
BIG1_HUMAN 1 .....MYEGKKTKNMFLTRALEKILADKEVKKAHHSQLRKACEVALEEIKAETEKQ
BIG2_HUMAN 1 .....MQESQTKSMFVSRALEKILADKEVKRPQHSQLRRACQVALDEIKAEIEKQ
GBF1_CRIGR 1 .....MVDKNIYIIQGEINIVVGAIKRNARWSTHIPLDE
GBF1_HUMAN 1 .....MVDKNIYIIQGEINIVVGAIKRNARWSTHTPLDE
GNOM_At 1 ...MGRLKLHSGIKAIEEEPEDFECTDSSNTTTLACMIDTEIAAVLAVMRRNVRWGGRYMSGDDQLEHSL
GEA1_YEAST 1 MHDVPMETVLAVNPATMIVKECINLCSAMNKQSRDKSQTSVAALLGGGSDIFLSQSDSFVDSFHNLPTSS
MON2p_HUMAN 1 .....MSGTSSPEAVKKLLENMQSDLRALSLECKKKFPPVKE
BIG1_HUMAN 52 SPPHGEA.KAGSSTLPPVKSKTNFIEADKYFLPFELACQSKCP..RIVSTSLDCLQKLIAYGHLTGNAPD
BIG2_HUMAN 51 ........RLGTAAPP....KANFIEADKYFLPFELACQSKSP..RVVSTSLDCLQKLIAYGHITGNAPD
GBF1_CRIGR 35 ERDPLLHSFSHLKEVLNSVTELSEIEPNVFLRPFLEVIRSEDTTGPITGLALTSVNKFLSYALIDPTHE.
GBF1_HUMAN 35 ERDPLLHSFGHLKEVLNSITELSEIEPNVFLRPFLEVIRSEDTTGPITGLALTSVNKFLSYALIDPTHE.
GNOM_At 68 IQSLKALRKQVFSWNQ....PWHTISPMLYLQPFLDVIRSDETGAPITSIALSSVYKILNLNVIDQNTA.
GEA1_YEAST 71 YHDPLISGLVQLRLKINDLKGLDSLNALELLKPFLEIVSASSVSGYTTSLALDSLQKVFTLKIINKTFN.
MON2p_HUMAN 38 AAESGIIKVKTIAARNTEILAALKENSSEVVQPFLMGCGTKEP..KITQLCLAAIQRLMSHEVVSETAA.
BIG1_HUMAN 119 STTPGKKLIDRIIETICGCFQG...PQTDEGVQLQIIKALLTAVTSQ.HIEIHEGTVLQAVRTCYNIYLA
BIG2_HUMAN 107 SGAPGKRLIDRIVETICSCFQG...PQTDEGVQLQIIKALLTAVTSP.HIEIHEGTILQTVRTCYNIYLA
GBF1_CRIGR 104 ...GTAEGMENMADAVTHARFVGTDPASDEVVLMKILQVLRTLLLTPVGTHLTNESVCEIMQSCFRICFE
GBF1_HUMAN 104 ...GTAEGMENMADAVTHARFVGTDPASDEVVLMKILQVLRTLLLTPVGAHLTNESVCEIMQSCFRICFE
GNOM_At 133 ...NIEDAMHLVVDSVTSCRFEVTDPASEEVVLMKILQVLLACMKNKASVMLSNQHVCTVVNTCFRVVHQ
GEA1_YEAST 140 ...DIQIAVRETVVALTHCRFEASKQISDDSVLLKVVTLLRDIITSSFGDYLSDTIIYDVLQTTLSLACN
MON2p_HUMAN 105 ...GNIINM.....LWQLMENSLEE...LKLLQTVLVLLTTNTV..VHDEALSKAIVLCFRLHFT
BIG1_HUMAN 185 SK..NLINQTTAKATLTQMLNVIFARMENQALQEAKQMEKER
BIG2_HUMAN 173 SK..NLINQTTAKATLTQMLNVIFTRMENQVLQEARRLEKPI
GBF1_CRIGR 171 MRL.SELLRKSAEHTLVDMVQLLFTRLPQFKEEPKSYVGTNM
GBF1_HUMAN 171 MRL.SELLRKSAEHTLVDMVQLLFTRLPQFKEEPKNYVGTNM
GNOM_At 200 AGMKGELLQRVARHTMHELVRCIFSHLPDVERTETTLVNRAG
GEA1_YEAST 207 TQR.SEVLRKTAEVTIAGITVKLFTKLKLLDPPTKTEKYIND
MON2p_HUMAN 157 K...DNITNNTAAATVRQVVTVVFERMVAEDERHRDIIEQPV
B
BIG1_HUMAN 557 ADAQSVVDIYVNYDCDLNAAN
BIG2_HUMAN 508 ADAQCVVDIYVNYDCDLNAAN
GBF1_CRIGR 528 RIPSFVTELYINYDCDYYCAN
GBF1_HUMAN 528 RIPSFVTELYINYDCDYYCSN
GEA1_YEAST 454 HSPAFFLQLFVNFDCNLDRSD
GNOM_At 455 RQKSFMVEMYANLDCDITCSN
C
Q0JU15_HUMAN 360 VQPQLLRSFCQSYDMKQHSTK
Q8K4V3_MOUSE 359 VQPQLLRSFCQSYDMKQHSTK
Q6GP04_XENLA 363 VQPQLLRSFCQSYDMKQHSTK
Q9VLT1_DROME 354 TRSSLIAFFCKSYDLKNHATN
Q19338_CAEEL 375 SSTDLVKWMTESFDCRPNSTH
YN37_YEAST 341 QDPEIVNTLYMDYDNYPDKKH
Q0JIX0_ORYSA 329 IEAHTLRLLFQTFDMNPTNTN

Figure 1

A

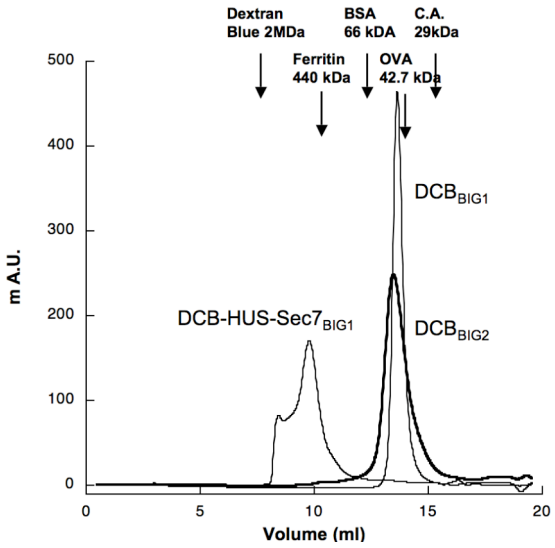
Dextran
Blue 2MDa
BSA
66 kDA
C.A.
29kDa
Ferritin
440 kDa
OVA
42.7 kDa
DCB$_{BIG1}$
DCB-HUS-Sec7$_{BIG1}$
DCB$_{BIG2}$
m A.U.
Volume (ml)

B

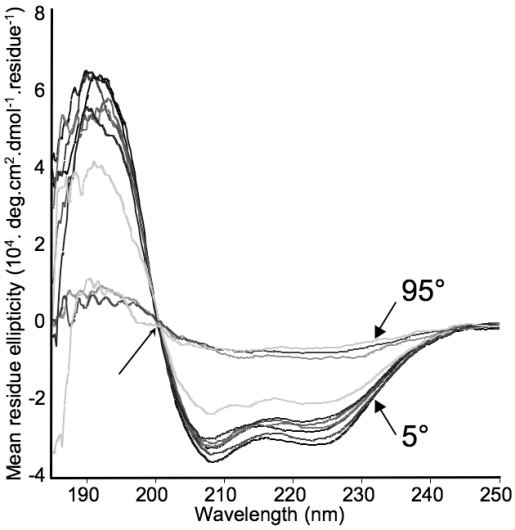
Mean residue ellipticity (10^4. deg.cm^2.dmol^{-1}.residue^{-1})
95°
5°
Wavelength (nm)

Figure 2

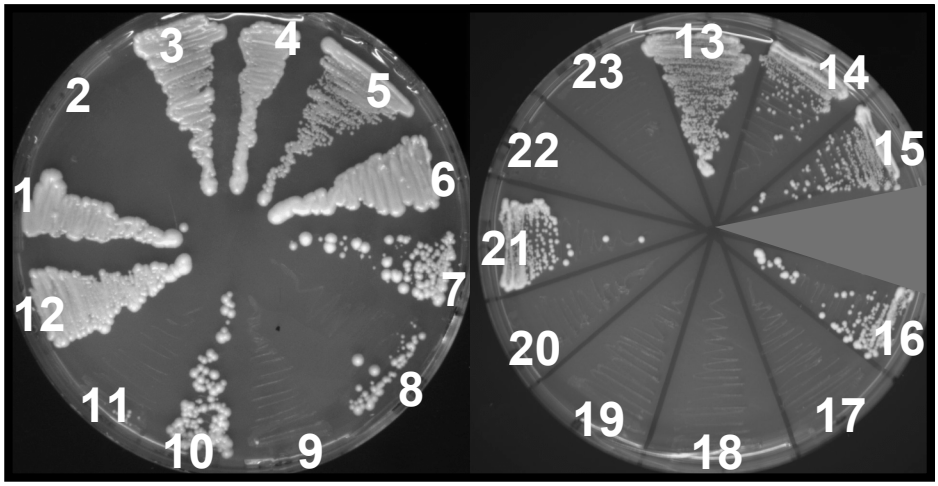

Figure 3

A

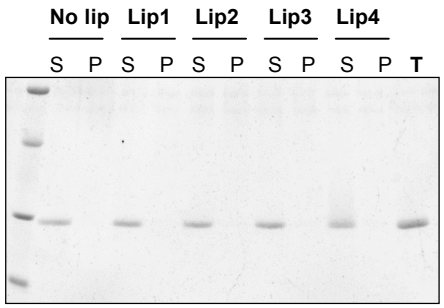
No lip
Lip1
Lip2
Lip3
Lip4
S P S P S P S P S P T

B

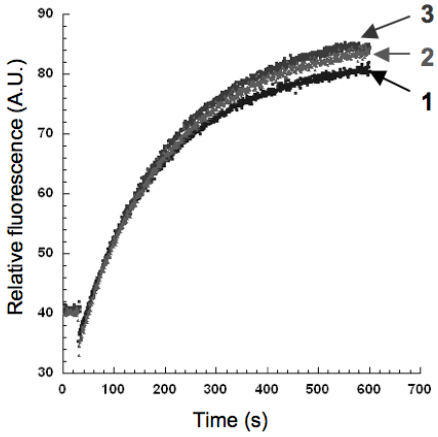
Relative fluorescence (A.U.)
Time (s)
3
2
1

C

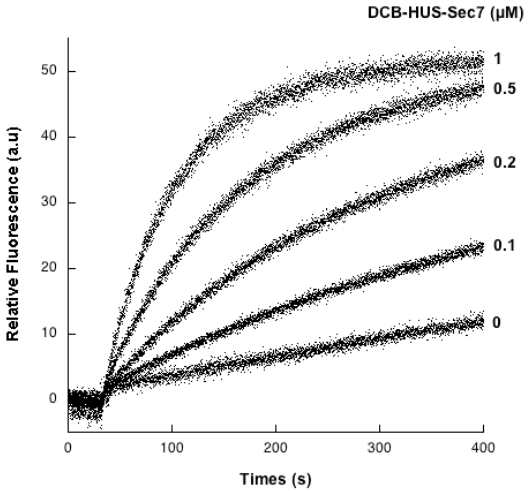
DCB-HUS-Sec7 (μM)
1
0.5
0.2
0.1
0
Relative Fluorescence (a.u)
Times (s)

Figure 4

A

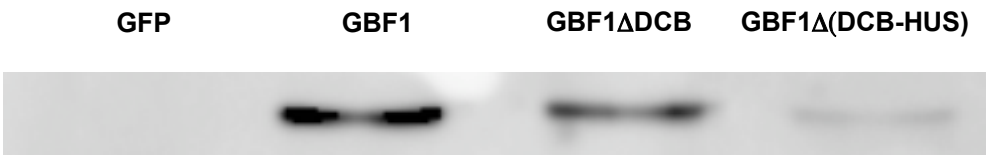
GFP
GBF1
GBF1ΔDCB
GBF1Δ(DCB-HUS)

B

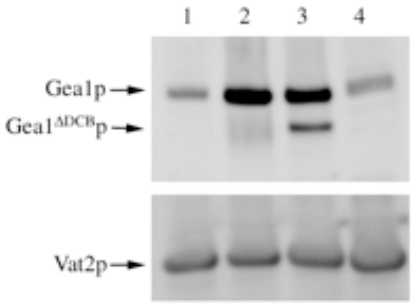
1
2
3
4
Gea1p
Gea1ΔDCBp
Vat2p

C

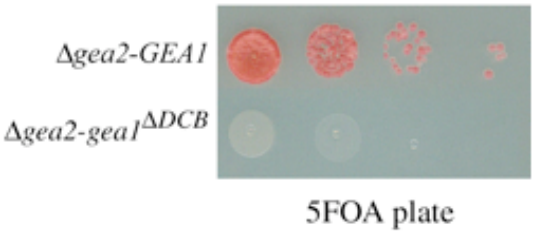
Δgea2-GEA1
Δgea2-gea1ΔDCB
5FOA plate

Figure 5

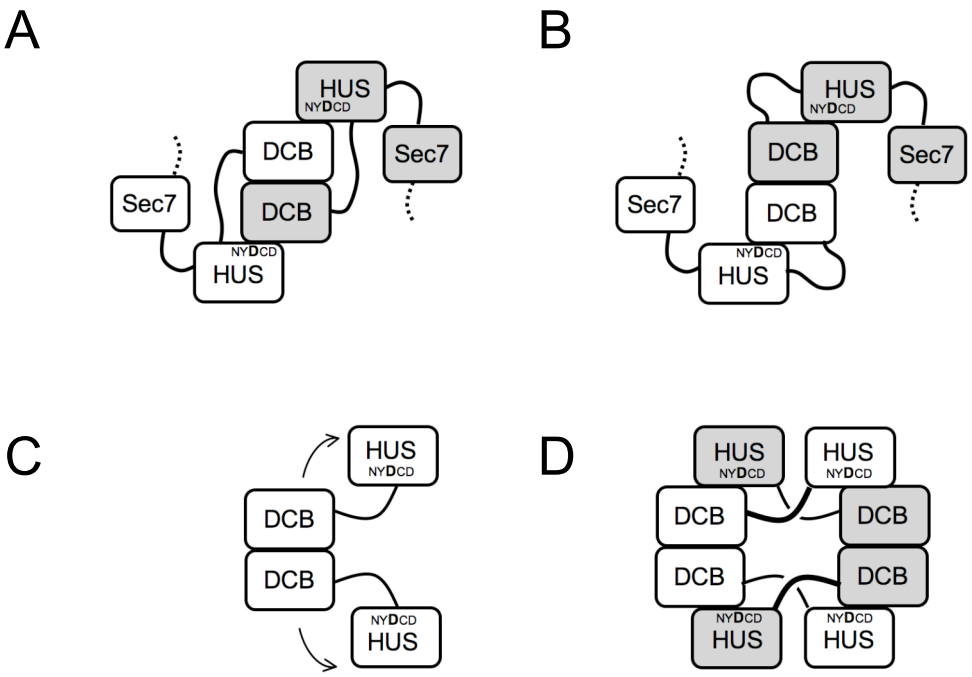
A
HUS
NYDCD
DCB
Sec7
Sec7
DCB
NYDCD
HUS
B
HUS
NYDCD
DCB
Sec7
Sec7
DCB
NYDCD
HUS
C
HUS
NYDCD
DCB
DCB
NYDCD
HUS
D
HUS
NYDCD
HUS
NYDCD
DCB
DCB
DCB
DCB
NYDCD
HUS
NYDCD
HUS

Figure 6